HNPS Advances in Nuclear Physics

Vol 30 (2024)

HNPS2023

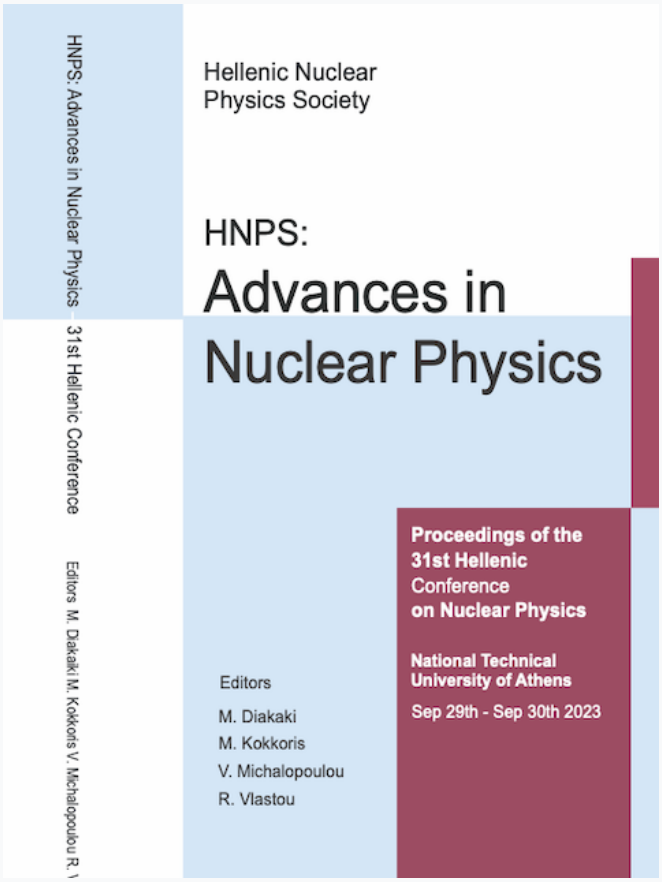

CFL quark stars as a candidate for the HESS J1731-347 object with a trace anomaly and GW190814 bound implementation

Pavlos Oikonomou, Ch.C. Moustakidis

doi: 10.12681/hnpsanp.6293

To cite this article:

Oikonomou, P., & Ch.C. Moustakidis. (2024). CFL quark stars as a candidate for the HESS J1731-347 object with a trace anomaly and GW190814 bound implementation. *HNPS Advances in Nuclear Physics*, *30*, 160–167. https://doi.org/10.12681/hnpsanp.6293

CFL quark stars as a candidate for the HESS J1731-347 object with a trace anomaly and GW190814 bound implementation

P.T. Oikonomou* and Ch.C. Moustakidis

Department of Theoretical Physics, Aristotle University of Thessaloniki, 54124 Thessaloniki, Greece

Abstract A recent analysis on the central compact object within HESS J1731-347 suggested unique mass and radius properties, rendering it a promising candidate for a self-bound star. In this present study, we examine the capability of quark stars composed of color-flavor locked quark matter to explain the latter object by using its marginalized posterior distribution and imposing it as a constraint on the relevant parameter space. The latter space is further confined due to the additional requirement for a high maximum mass ($M_{TOV} \geq 2.6\, M_{\odot}$), accounting for GW190814's secondary companion. Critical emphasis is placed on the speed of sound and the trace anomaly which was proposed as a measure of conformality [Y. Fujimoto et al., Phys. Rev. Lett. 129, 252702 (2022)]. We conclude that color-flavor locked quark stars can reach high masses without violating the conformal or the $\langle\Theta\rangle_{\mu_B} \geq 0$ bound ($\langle\Theta\rangle_{\mu_B}$ being the non-normalized trace anomaly at vanishing temperatures), provided that the quartic coefficient α_4 (a crucial parameter accounting for pQCD corrections in the matter's thermodynamic potential) does not exceed an upper limit which depends on the established M_{TOV}. For $M_{TOV} = 2.6M_{\odot}$, we find that the limit reads $\alpha_4 \leq 0.594$. Lastly, a final investigation takes place on the agreement of colour-flavour locked quark stars with additional astrophysical objects including the GW170817 and GW190425 events, followed by some concluding remarks.

Keywords color-flavor locked quark matter, quark stars, HESS J1731-347, GW190814, trace anomaly

INTRODUCTION

A substantial amount of activity has been focused on Witten's proposal regarding the true ground state of matter [1]. The hypothesis of quark matter consisting of u, d, and s quarks, also called strange matter, having an energy per baryon lower than that of nuclear matter and u, d quark matter, along with the expectation of deconfined quark matter at high densities [2,3], has lead to the study of an exotic outcome called strange stars . Such objects, due to their nature, can reach arbitrarily small radii and masses [3].

Later work has shown that the aforementioned matter should be a color superconductor, a degenerate Fermi gas in which the quarks near the Fermi surface form Cooper pairs, breaking the color gauge symmetry [4-6]. At asymptotically high densities, the most favorable state for strange quark matter is the color-flavor-locked (CFL) phase, a superfluid which furthermore breaks chiral symmetry, where quarks of all three flavors and colors pair with each other in a correlated way [4-6].

A recent analysis on the supernova remnant HESS J1731-347 suggests that the mass and radius of the central compact object within it are $M = 0.77^{+0.20}_{-0.17}\, M_{\odot}$ and $R = 10.4^{+0.86}_{-0.78}$ km respectively [7]. This estimation is rather intriguing. Considering that a previous analysis by Suwa et al. [8] indicated that the minimum possible mass of a neutron star is $1.17M_{\odot}$, it raises the question of whether the compact object in HESS J1731-347 could be an exotic one rather than a neutron star. We furthermore turn our attention to the secondary companion of the notable GW190814 event [9] which is a compact object with a mass of 2.50−2.67M⊙ (measurement reported at the 90% credible level). In this study, we also explore the possibility that the aforementioned object could be a CFL quark star and we investigate the implications of this conjecture on CFL quark matter and the associated parameter space; our prime goal is to present the capability of CFL quark stars to explain the HESS J1731 − 347 compact object, as well

* Corresponding author: *p.th.oikonomou@gmail.com*

as objects with masses equal or greater than that of GW190814's secondary companion [9] without violating the conformal limit ($u_s^2 \rightarrow 1/3$) or the positive trace anomaly bound proposed in [10].

PROPERTIES OF CFL QUARK MATTER

In this research, we will be utilizing the EoS derived in [11] under an MIT bag model formalism. This EoS represents the interior of strange stars composed of CFL quark matter and reads

$$\varepsilon_{CFL} = 3P + 4B_{eff} + \frac{3w^2}{4\pi^2} + \frac{w}{\pi}\sqrt{3\left(P + B_{eff}\right) + \frac{9w^2}{16\pi^2}}. \quad (1)$$

where P is the pressure, B_{eff} the effective bag constant representing the nonperturbative QCD vacuum effects and $w = (m_s^2 - 4\Delta^2)/\sqrt{\alpha_4}$. In the latter equation, m_s represents the mass of the strange quark which is fixed at 95 MeV throughout this study, Δ represents the gap of the CFL quark pairing and the quartic coefficient α_4 represents the p(erturbative)QCD corrections.

The respective energy per baryon number E/A relation of this matter reads

$$\left(E/A\right)_{CFL} = \frac{2\sqrt{6}\pi}{k^{1/2}} \frac{B_{eff}^{1/2}}{\sqrt{\sqrt{\frac{16\pi^2}{3}B_{eff} + w^2} - w}}, \quad (2)$$

where $k = \sqrt{\alpha_4}$. Eq. (2) is crucial for the stability examination of the CFL quark matter.

OBSERVATIONAL CONSTRAINTS

For the proper investigation of the compatibility of CFL quark stars with the HESS J1731-347 remnant and the secondary companion of the GW190814 event, appropriate constraints regarding the stability of the CFL quark matter as well as the measurements of the aforementioned objects need to established. The first constraint concerns the utter stability of the CFL phase having an energy per baryon $E/A \leq 930$ MeV, where 930 MeV is roughly the energy per baryon of the most stable nucleus ${}^{56}_{26}Fe$. The second one concerns the observed stability of ordinary nuclei and the absence of their decay to u, d quark droplets. This term thus corresponds to the energy per baryon of unpaired u, d (ud) quark matter and reads $(E/A)_{ud} \geq 934$ MeV, where we have added 4 MeV due to surface effects [12].

We now narrow our focus on the marginalized posterior distribution of HESS J1731-347's central compact object (excluding all additional priors described on the text) which reads $M = 0.77^{+0.20}_{-0.17}\, M_\odot$ and $R = 10.4^{+0.86}_{-0.78}$ km [7]. By performing a series of cubic spline interpolations we imported robust limitations on the parameter space, corresponding to the latter object, by establishing $R_{0.97min} = 9.62$ km and $R_{0.6max} = 11.26$ km on the radii of CFL quark stars, producing the corresponding lines in Fig. 3. This particular choice of constraints is guided by the form of the M−R curves, depicted in Fig.4. It is evident that the lower right ($R_{0.6} = 11.26$ km) and upper left ($R_{0.97} = 9.62$ km) limits of the aforementioned posterior distribution (indicated by the yellow area in the figure) exclusively constrain the M − R curves of CFL quark stars. By further considering the M − R graph behavior, which is determined by Eq. (1), we have ensured the validity of this formalism with no exceptions. Furthermore, we perform additional interpolations for the constraints related to the GW190814 event which we translate to a maximum mass bound of $M_{TOV} \geq 2.6 M_\odot$, producing once more the corresponding lines on the parameter space. Due to the finding of [13,14,15], we take as an example two different cases of the quartic coefficient $a_4 = 0.65$, 0.75 and by incorporating the stability constraints mentioned above, we depict our overall results in Fig. 1. For comparison, we also depict the constraint for the utter stability ($E/A \geq 930$ MeV) of the 2SC phase. The latter is a charge-neutral colour-superconducting phase consisting of paired u,d massless quarks with an energy per baryon relation reading [11]

$$\left(E/A\right)_{2SC} = \frac{3\sqrt{2}\pi B_{eff}^{1/2}}{\sqrt{\sqrt{c\pi^2 B_{eff} + \Delta^4} + \Delta^2}},$$

with $c = [3^{-\frac{4}{3}}\left(1 + 2^{\frac{4}{3}}\right)]^{-3}k^2$. Our focus however will be solely fixed in the CFL phase.

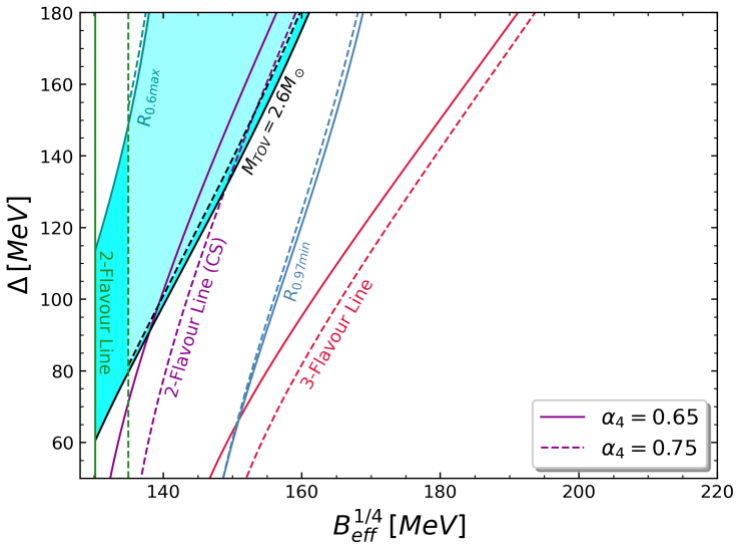

Figure 1. *The 2-D parameter space $\Delta - B_{eff}^{1/4}$ with applied observational constraints for two different values of α_4 and fixed m_s = 95 MeV. On the left of every utter stability line, the corresponding matter is more stable than nuclear matter while the astrophysical bounds indicate the appropriate regions that allow for the explanation of the respective object as CFL quark stars; black for the GW190814 event ($M_{TOV} \geq 2.6M_\odot$) and blue for the marginalized constraints of the HESS J1731–347 remnant ($R_{0.97min} = 9.62$ km and $R_{0.6max} = 11.26$ km). The vivid light blue area represents the window of the parameter space inside of which both of the aforementioned objects can be explained for α_4 = 0.65, while the frail shade corresponds to both (α_4 = 0.65 and α_4 = 0.75) cases. The green lines serve as a limit for the surety of the favor of ordinary nuclei over neutral unpaired u, d quark matter, making the two-dimensional parameter space left of them forbidden.*

TIDAL DEFORMABILITY

A very important source for the gravitational wave detectors is the gravitational waves from the late phase of the inspiral of a binary compact star system, before the merger [16-17]. This kind of source leads to the measurement of various properties of compact stars. In the inspiral phase the tidal effects can be detected [17]. The k_2 parameter, also known as tidal Love number, depends on the equation of state and describes the response of a compact star to the tidal field E_{ij} [17]. The exact relation reads

$$Q_{ij} = -\lambda E_{ij}, \quad (3)$$

where $\lambda = 2R^5 k_2/3G$ and R is the star's tidal deformability and radius respectively. The former can be written in a dimensionless form as follows

$$\Lambda = \frac{2}{3}k_2\left(\frac{R}{GM}\right)^5. \quad (4)$$

Lastly, we will be also studying the average tidal deformability of a binary system which is defined as [3]

$$\tilde{\Lambda} = \frac{16}{13}\frac{(M_1 + 12M_2)M_1^4\Lambda_1 + (M_2 + 12M_1)M_2^4\Lambda_2}{(M_1 + M_2)^5}. \quad (5)$$

By accounting for the energy discontinuity in the surface of bare quark stars [3] we can exploit the equations depicted above and gain valuable knowledge about the tidal properties of a star and a binary system and compare them with the restrictions induced by several gravitational wave events.

SPEED OF SOUND AND TRACE ANOMALY

In this section, the scrutiny of the speed of sound is presented in response to the causality ($u_s \leq 1$) and the conformal ($u_s \leq 1/\sqrt{3}$) limit. The aforementioned quantity is defined as

$$\frac{1}{u_s^2} = \frac{d\mathcal{E}}{dP} = 3 + \frac{3w}{2\pi\sqrt{3\left(P + B_{eff}\right) + \frac{9w^2}{16\pi^2}}}, \tag{6}$$

and it is evident that in $w \geq 0$ space, neither of the limits is violated, whereas in the $w < 0$ space the speed of sound does violate the conformal limit $\forall\, B_{eff} > 0$ and $w < 0$. Our results are depicted in Fig. 2 for various $\Delta - B_{eff}$ pairs.

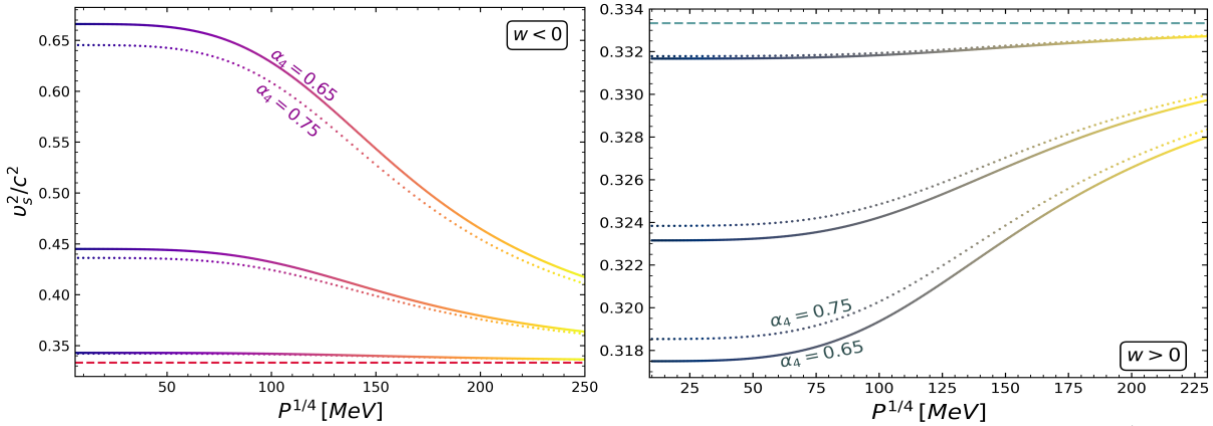

Figure 2. *The speed of sound as a function of the pressure in the w < 0 space (left) for* $\{\Delta = 60\ MeV, B_{eff}^{1/4} = 148\ MeV\}, \{\Delta = 120\ MeV, B_{eff}^{1/4} = 143\ MeV\}$ *and* $\{\Delta = 180\ MeV, B_{eff}^{1/4} = 135\ MeV\}$ *along with the w > 0 case (right) for* $\{\Delta = 16\ MeV, B_{eff}^{1/4} = 135\ MeV\}$, $\{\Delta = 30\ MeV, B_{eff}^{1/4} = 140\ MeV\}$, *and* $\{\Delta = 45\ MeV, B_{eff}^{1/4} = 145\ MeV\}$. *The pairs in each case are depicted from bottom to top respectively and the dashed lines represent the same limit* $u_s^2 \to 1/3$. *Each of these pairs also satisfy the two stability constraints mentioned in the second section.*

A recently conducted research [10], which proposes the trace anomaly as a measure of conformality, demonstrated that the speed of sound in the case of neutron stars does not violate the conformal bound when $u_s^2 > 1/3$, but it displays a steep approach to the conformal limit. In particular, the speed of sound is expressed solely in terms of the (normalized) trace anomaly and it is suggested that the latter is a more comprehensive quantity than u_s. The quantity is defined as

$$\mathcal{D} \equiv \frac{\langle\Theta\rangle_{T,\mu_B}}{3\mathcal{E}} = \frac{1}{3} - \frac{P}{\mathcal{E}}, \quad \langle\Theta\rangle_{T,\mu_B} = \mathcal{E} - 3P. \tag{7}$$

In this instance, $\langle\Theta\rangle_{T,\mu_B}$ is the matter part of the trace of the energy-momentum tensor, the normalized trace anomaly has to satisfy the constraints $-2/3 \leq \mathcal{D} \leq 1/3$. It is furthermore suggested that there may be a positive bound on the trance anomaly reading $\langle\Theta\rangle_{\mu_B} \geq 0$ for cold dense matter. We study this case and find that in the $w < 0$ space a violation is possible if the following relation is infringed by the pressure of CFL quark matter

$$B_{eff}^2 \geq \frac{3w^2}{16\pi^2}\left(P - B_{eff}\right). \tag{8}$$

It is clear that no violation occurs in the $w \geq 0$ space. These results are presented in Fig. 3 for the normalised trace anomaly $\mathcal{D}$ as a function of the energy density $\mathcal{E}$.

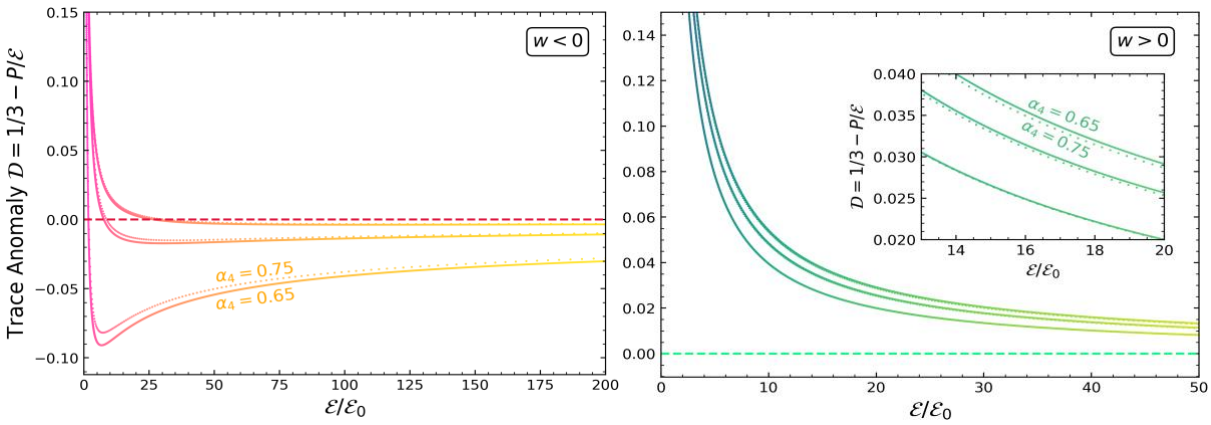

Figure 3. *The trace anomaly as a function of the energy density (normalized to the value of the saturation energy density* $\mathcal{E}_0^{1/4} = 184.25\ MeV$*),* $\{\Delta = 85\ MeV, B_{eff}^{\frac{1}{4}} = 135.84\ MeV\}, \{\Delta = 120\ MeV, B_{eff}^{1/4} = 143\ MeV\}$*, and* $\{\Delta = 180\ MeV, B_{eff}^{1/4} = 138\ MeV\}$ *in* $w < 0$ *and* $\{\Delta = 16\ MeV, B_{eff}^{1/4} = 140\ MeV\}$, $\{\Delta = 30\ MeV, B_{eff}^{1/4} = 138\ MeV\}, \{\Delta = 45\ MeV, B_{eff}^{1/4} = 135\ MeV\}$ *in w > 0. The dashed lines in this case represent the limit induced from the* $\langle\Theta\rangle_{\mu_B} \geq 0$ *bound while the pairs are depicted from top to bottom. Each presented pair satisfies the stability constraints mentioned in the second section while the utilized w < 0 pairs of the lower panel additionally lie within the frail blue window of Fig. 1.*

It is concluded that in the w < 0 space violations occur in both of the scenarios examined above, contrary to the w ≥ 0 case. The latter range (and thus small Δ) is also favored due to high temperatures on the surface of the HESS J1731-347 remnant as explained by J.E. Horvath et al. in [18] (see also the work of F. Di Clemente et al. in [19]). An additional theoretical justification for the w ≥ 0 preference arises from the results of the second section and specifically Fig. 1. As one can see positive w values are associated with small B_{eff} values which favor the existence of CFL quark starts and discourage the formation of hybrid stars, as demonstrated in [20]. We thus focus in this instance by lowering the quartic coefficient a_4 until the objects of interest can be described by gap values in the w ≥ 0 space. For the constraints concluded in the second section, the limit placed on the quartic coefficient is about $a_4 \leq 0.594$, independent of the strange quark's mass value ms. The sole role on the derivation of this bound lies within the MTOV ≥ 2.6$M_\odot$ constraint as one can see from Fig. 3. Thus, one can establish a lower limit to gain a higher limit on α4 and vice versa (for MTOV ≥ 2.5$M_\odot$ the limit reads $\alpha_4 \leq 0.643$).

ADDITIONAL OBSERVATIONAL CONSTRAINTS

In this section we study the further compliance of CFL quark stars that obey the constraints depicted in Fig.1 with additional observational phenomena. In the following, we take into account two different values of the quartic coefficient $\alpha_4 = 0.65$ and $\alpha_4 = 0.55$ and examine the properties of such stars. The choice of the latter value is based on the findings of [18] and the conclusions of latter section, where violations on the speed of sound and the trace anomaly for w < 0 were depicted. These findings encourage us to consider α4 values that allow for the utilization of the w ≥ 0 space. In Fig. 4, we depict numerous M-R graphs along with the characteristics of several astrophysical objects [7,9,21-26] and the GW170817 event [27]. Even though a number of CFL quark stars satisfy the constraints established be the 2-d posterior of the GW170817 event, they are not soft enough to satisfy the corresponding tidal constraints. To be more precise, we find that the gap threshold needed to achieve such softness exceeds 200 MeV and is depicted in the table below with respect to different a_4 values. We note that gap values above or equal to the threshold do not construct the desirable softness with any effective bag value. Rather, since our stars satisfy the constraints of Fig. 1, the thresholds translate to the minimum possible

gap that can be utilized with certain effective bag values to produce the wanted softness. The minimum bag parameter is also mentioned below.

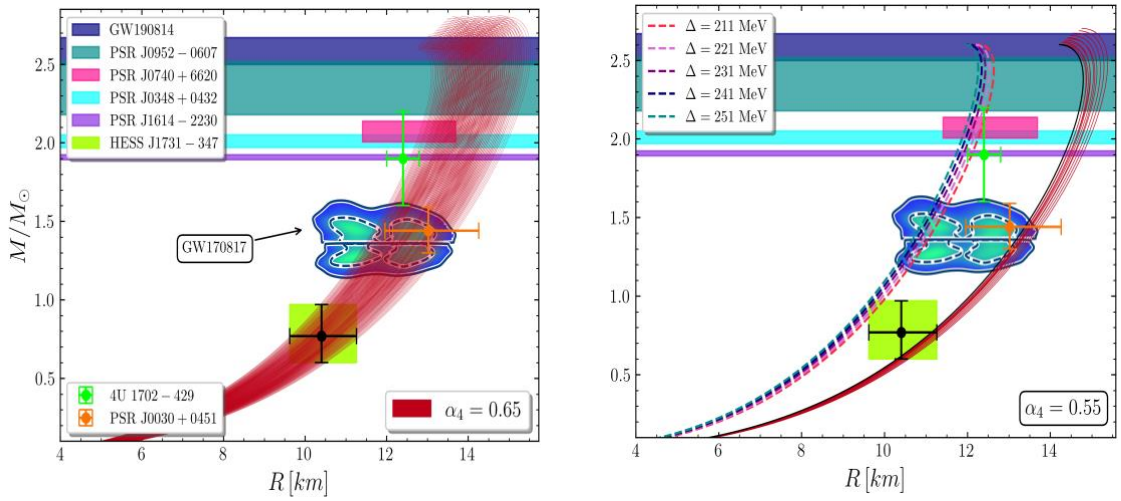

Figure 4.*Mass-Radius relations of CFL quark stars for (Left panel)* $a_4 = 0.65$ *and various* $\Delta - Beff$ *pairs* ($\Delta \in [80, 180]$ *MeV and* $B_{eff}^{1/4} \in [130.6, 161]$ *MeV) that satisfy the constraints deduced in Sec. III. (Right panel)* $\alpha 4 = 0.55$ *and several* $\Delta - Beff$ *pairs that also satisfy the aforementioned limits, with the red solid lines additionally lying within the* $w \geq 0$ *space* ($\Delta \in [35.5, 47.5]$ *MeV and* $B_{eff}^{1/4} \in [124.87, 127.32]$ *MeV), and the coloured dashed ones being consistent with the GW170817 and GW190425 tidal constraints* ({$\Delta = 211$ *MeV,* $B_{eff}^{1/4} = 169.08$ *MeV*},{$\Delta = 221$ *MeV,* $B_{eff}^{1/4} = 170.94$ *MeV*},{$\Delta = 231$ *MeV,* $B_{eff}^{1/4} = 172.66$ *MeV*},{$\Delta = 241$ *MeV,* $B_{eff}^{1/4} = 174.25$ *MeV*} *and* {$\Delta = 251$ *MeV,* $B_{eff}^{1/4} = 175.75$ *MeV*}). *The black solid line represents the softest EoS possible in the* $w \geq 0$ *space with* [$\Delta = 47.5$, $B_{eff}^{1/4} = 127.32$] *MeV. From top to bottom, the coloured bands correspond to measurements of, GW190814's secondary companion [7], PSR J0952-0607 [21], PSR J0740+6620's marginalised posterior distribution [22], PSR J0348+0432 [23], PSR J1614-2230 [24], GW170817 (solid and dashed lines represent the 90% and 50% credible level respectively) [27] and HESS J1731-347's marginalised distribution [9]. The error bars with null background represent the marginalised distributions of 4U 1702 − 429 [25] and PSR J0030+0451 [26] correspondingly.*

It is therefore concluded that the $w \geq 0$ space cannot explain the GW170817 event. Furthermore, by testing the softest possible EoS in the aforementioned space which occurs at w=0 (indepdent of α_4), for different established M_{TOV}, we conclude that GW190425 [28] cannot be explained either. Our results regarding the tidal properties of the two events are depicted in Fig. 5.

Table 1. *Minimum possible values of the gap Δ needed in order for CFL quark stars to additionally satisfy the total tidal constraints of the GW170817 event, for three different α4 values. These constraints are also depicted in Figs.5 and 6. The respective minimum effective bag parameter is about* $B_{eff}^{1/4} = 168.94$ *MeV, for every* a_4.

a_4	Δ_{min} (MeV)
0.55	210.29
0.65	218.87
0.75	226.38

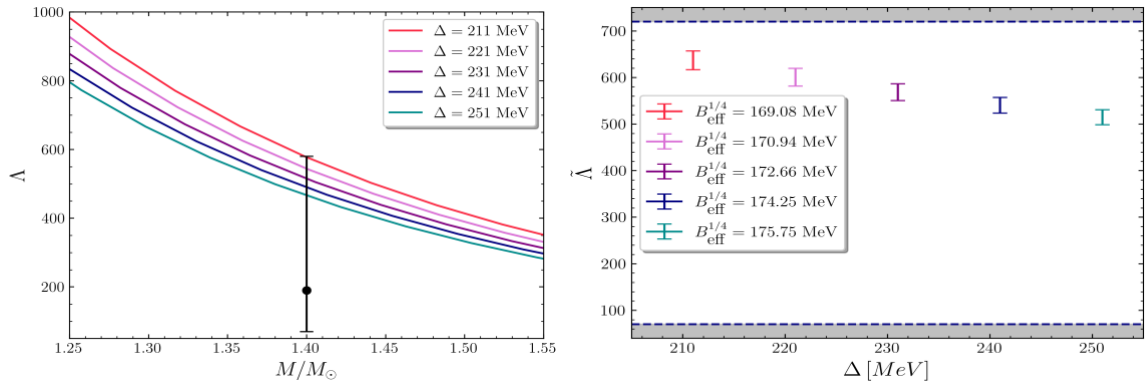

Figure 5. *The compliance of CFL quark stars with the GW170817 merger. Left panel: Dimensionless tidal deformability Λ as a function of the normalised mass $M/M_{\odot}$, adjusted at $1.4M_{\odot}$. The error bar represents the $\Lambda_{1.4} = 190^{+390}_{-120}$ constraints concluded by the LVC [27]. Right panel: The average tidal deformability $\tilde{\Lambda}$ for different parametrizations. The dashed lines indicate the limits of the $\tilde{\Lambda} = 300^{+420}_{-230}$ constraint [29]. The utilised $\Delta - Beff$ pairs are identical to the ones from Fig. 4(b).*

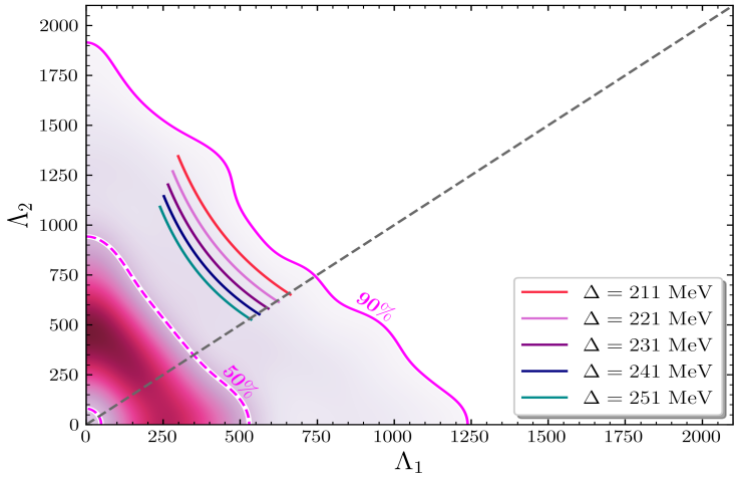

Figure 6. *Λ1 − Λ2 relation for the parameters utilized in Figs. 4(b) and 5. The 50% and 90% credible lines correspond to the GW170817 event and are obtained from [27].*

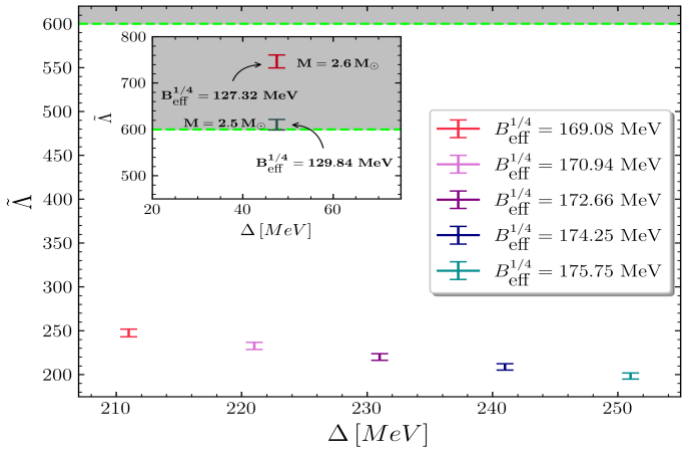

Figure 7. *The average tidal deformability $\tilde{\Lambda}$ for different parametrizations. The dashed line represents the $\tilde{\Lambda} \leq 600$ constraint of the GW190425 event concluded by the LVC [28]. Parameter pairs that lie within the confined window correspond to the same pairs that were utilized in Fig. 5, while the two remaining pairs correspond to the softest possible EoS that utilizes $w \geq 0$ parameters, for two different established $M_{TOV} = 2.5, 2.6M_{\odot}$.*

CONCLUSIONS

In this study we aimed to explain the central compact object inside the HESS J1731-347 remnant as a CFL quark stars by also establishing a high mass bound for the secondary companion in the GW190814 event and a positive trace anomaly constraint. We reached to the conclusion that such a scenario is possible inside the $w \geq 0$ space where the superconducting gap cannot take values larger than $m_s/2$. This space is not only observationaly favourable due to some recent studies regarding the surface temperature of the object in interest, but also theoreticaly due to the respective small bag values that we can utilise. However, we conclude that CFL quark stars inside this space are not able to (effectively) explain two important gravitational wave events; GW170817 and GW190425. Future observations and findings will surely shed light to our results.

References

[1] E. Witten, Phys. Rev. D 30, 272 (1984); doi: 10.1103/PhysRevD.30.272
[2] F. Weber, Prog. Part. Nucl. Phys. 54, 193 (2005); doi: 10.1016/j.ppnp.2004.07.001
[3] J. Schaffner-Bielich, Compact Star Physics (Cambridge University Press, Cambridge, England, 2020)
[4] M.G. Alford, Annu. Rev. Nucl. Part. Sci. 51, 131 (2001); doi: 10.1146/annurev.nucl.51.101701.132449
[5] M.G. Alfordet al., Rev. Mod. Phys. 80, 1455 (2008); doi: 10.1103/RevModPhys.80.1455
[6] K. Rajagopal and F. Wilczek, The condensed matter physics of QCD, in At the Frontier of Particle Physics. Handbook of QCD, (World Scientific, Singapore, 2000), Vol. 1–3, pp. 2061–2151
[7] V. Doroshenko, et al., Nat. Astron. 6, 1444 (2022); doi: 10.1038/s41550-022-01800-1
[8] Y. Suwa et al., Mon. Not. R. Astron. Soc. 481, 3305 (2018); doi: 10.1093/mnras/sty2460
[9] R. Abbott et al., Astrophys. J. Lett. 896, L44 (2020); doi: 10.3847/2041-8213/ab960f
[10] Y. Fujimoto et al., Phys. Rev. Lett. 129, 252702 (2022)l doi: 10.1103/PhysRevLett.129.252702
[11] P.T. Oikonomou, Ch.C. Moustakidis, Phys. Rev. D 108, 063010 (2023); doi: 10.1103/PhysRevD.108.063010
[12] E. Farhi and R.L. Jaffe, Phys. Rev. D 30, 2379 (1984); doi: 10.1103/PhysRevD.30.2379
[13] M. Alford et al., Astrophys. J. 629, 969 (2005); doi: 10.1086/430902
[14] E.S. Fraga et al., Phys. Rev. D 63, 121702 (2001); doi: 10.1103/PhysRevD.63.121702
[15] Z. Miao et al., Astrophys. J. 917, L22 (2021); doi: 10.3847/2041-8213/ac194d
[16] S. Postnikov et al., Phys. Rev. D 82, 024016 (2010); doi: 10.1103/PhysRevD.82.024016
[17] E.E. Flanagan and T. Hinderer, Phys. Rev. D 77, 021502(R) (2008); doi: 10.1103/PhysRevD.77.021502
[18] J.E. Horvath et al., Astron. Astrophys. 672 L11 (2023); doi: 10.1051/0004-6361/202345885
[19] F. Di Clemente, A. Drago, and G. Pagliara, arXiv:2211 .07485
[20] M. Alford and S. Reddy, Phys. Rev. D 67, 074024 (2003); doi: 10.1103/PhysRevD.67.074024
[21] R.W. Romani et al., Astrophys. J. Lett. 934, L17 (2022); doi: 10.3847/2041-8213/ac8007
[22] T.E. Riley et al., Astrophys. J. Lett. 918, L27 (2021); doi: 10.3847/2041-8213/ac0a81
[23] J. Antoniadis et al., Science 340, 448 (2013); doi: 10.1126/science.1233232
[24] Z. Arzoumanian et al., Astrophys. J. Suppl. Ser. 235, 37 (2018); doi: 10.3847/1538-4365/aab5b0
[25] J. Nättilä et al., Astron. Astrophys. 608, A31 (2017); doi: 10.1051/0004-6361/201731082
[26] M.C. Miller et al., Astrophys. J. Lett. 887, L24 (2019); doi: 10.3847/2041-8213/ab50c5
[27] B.P. Abbott et al., Phys. Rev. Lett. 121, 161101 (2018); doi: 10.1103/PhysRevLett.121.161101
[28] B.P. Abbott et al., Astrophys. J. Lett. 892, L3 (2020); doi: 10.3847/2041-8213/ab75f5
[29] B.P. Abbott et al., Phys. Rev. X 9, 011001 (2019); doi: 10.1103/PhysRevX.9.011001